Peculiar Effects of Anisotropic Diffusion on Dynamics of Vicinal Surfaces

G. Danker,[1] O. Pierre-Louis,[2] K. Kassner,[1] and C. Misbah[2]

[1]*Institut für Theoretische Physik, Otto-von-Guericke-Universität Magdeburg, Postfach 4120, D-39016 Magdeburg, Germany*
[2]*Spectro, CNRS, UMR5588, Université J. Fourier, Grenoble 1, BP87, F38402 Saint Martin d'Hères, France*

(Received 1 April 2004; published 29 October 2004)

We report on peculiar behaviors due to anisotropic terrace diffusion on step meandering on a vicinal surface. We find that anisotropy triggers tilted ripples. In addition, if the fast diffusion direction is perpendicular to the steps, the instability is moderate and coarsening is absent, while in the opposite case the instability is promoted, and interrupted coarsening may be observed. Strong enough anisotropy restabilizes the step for almost all step orientations. These findings point to the nontrivial effect of anisotropy and open promising lines of inquiries in the design of surface architectures.

DOI: 10.1103/PhysRevLett.93.185504 PACS numbers: 81.10.Aj, 68.35.Ct, 81.15.Hi

Molecular beam epitaxy (MBE) is often used to design high quality nanostructures on vicinal surfaces. The occurrence of instabilities on these surfaces, and pattern formation in general, confers to vicinal surfaces a great potential as template for self-assemblies of nanoscale devices [1]. Surface instabilities and pattern formation during MBE are naturally described in terms of dynamics of crystal steps. So far, most of the theoretical treatments have focused on isotropic situations, mainly for simplicity reasons (with some exceptions; see, e.g., Ref. [2]). Anisotropy is, however, ubiquitous and must be taken into account with the aim of confronting theoretical results with more realistic situations. It may originate from the symmetry of the substrate or from surface reconstructions. The sources of anisotropy are mainly twofold: (i) surface diffusion anisotropy and (ii) anisotropy of step properties, such as the stiffness. Both are believed to play a central role in the pattern formation process. For example, anisotropy has been found to promote ripple formation during homoepitaxy on anisotropic substrates [3]. In another context, namely, in the submonolayer regime, the spatial distribution of two dimensional islands is found to strongly depend on the anisotropy of the substrate [4].

Here we report on peculiar behaviors of terrace diffusion anisotropy and its impact on step meandering. The main results reported here are as follows. (i) In contrast to the case where either the step stiffness or step edge diffusion are anisotropic, we find that terrace diffusion anisotropy may lead to tilted meandering ripples. (ii) If the fast diffusion axis is perpendicular to the steps, the instability is weaker (i.e., larger time scales and larger wavelength) and does not exhibit coarsening. (iii) If the fast diffusion direction is along the steps, the instability is stronger, and interrupted coarsening is found. (iv) When anisotropy is very strong, the instability is weaker for most orientations, except if the fast diffusion axis is almost perfectly aligned with the steps. We shall also show that the anisotropic diffusion model can be mapped onto a model with isotropic terrace diffusion, but with new effective anisotropic step properties. This mapping significantly simplifies the analysis.

Let us briefly describe the basic step model with anisotropic terrace diffusion, and anisotropic step properties (Fig. 1). The motion of adatoms on terraces is governed by the diffusion law,

$$\mathbf{j} = -\underline{\underline{D}}\nabla c, \tag{1}$$

which links the mass current $\mathbf{j}$ to the adatom concentration c. The diffusion tensor

$$\underline{\underline{D}} = \begin{pmatrix} D_{11} & D_{12} \\ D_{12} & D_{22} \end{pmatrix} \tag{2}$$

describes the anisotropy of terrace diffusion. Mass conservation on terraces reads

$$\partial_t c = F - \nabla \cdot \mathbf{j}. \tag{3}$$

We assume that desorption is negligible, which is usually the case in MBE.

At the steps, the adatom mass current is linked to the linear departure from equilibrium, with kinetic coefficients $\nu_{\pm}$:

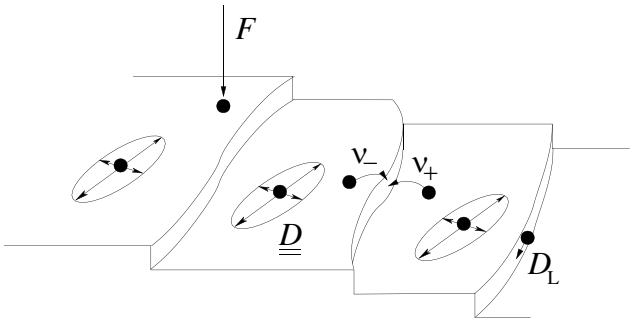

FIG. 1. Sketch of a vicinal surface. The fundamental processes that contribute to the growth of the crystal are shown: attachment to the surface (F), diffusion on the terrace ($\underline{\underline{D}}$) and along the steps ($D_L$), and attachment to the step from the lower terrace (ν_+) and from the upper terrace (ν_-).

$$\mp \mathbf{n} \cdot \mathbf{j}|_{\pm} = \nu_{\pm}(c - c_{\mathrm{eq}})|_{\pm}. \quad (4)$$

Here $\mathbf{n}$ is the normal to the step (pointing to the lower terrace). The equilibrium concentration c_{eq} at a step is determined by the Gibbs-Thomson relation:

$$c_{\mathrm{eq}} = c_{\mathrm{eq}}^0(1 + \Gamma\kappa), \quad (5)$$

with $\Gamma = \Omega\tilde{\gamma}/k_BT$, where $\tilde{\gamma}$ is the step stiffness. κ is the local curvature. The + sign refers to the ascending and the − sign to the descending side of the step.

Finally, mass conservation at the step determines the step velocity:

$$v_n = \Omega\mathbf{n} \cdot (\mathbf{j}|_- - \mathbf{j}|_+) + a\partial_s[D_L\partial_s(\Gamma\kappa)]. \quad (6)$$

Ω is the atomic area and a the lattice constant. D_L is the macroscopic diffusion constant that describes the diffusion of adatoms along the step. The operator ∂_s denotes differentiation along the step. The kinetic coefficients $\nu_{\pm}$, D_L, and the step stiffness $\tilde{\gamma}$ are anisotropic quantities, which depend on the local orientation of the step.

We introduce a geometrical mapping which allows one to reduce the step model to a model with isotropic terrace diffusion. For that purpose we make use of the following transformation:

$$\bar{x} = x - \frac{D_{12}}{D_{22}}z, \qquad \bar{z} = \frac{D_0}{D_{22}}z, \quad (7)$$

where we have set $D_0 = [D_{11}D_{22} - D_{12}^2]^{1/2}$ for brevity. Equation (7) maps the Cartesian coordinates (x, z) onto new coordinates $(\bar{x}, \bar{z})$ and thus the step curve $\mathbf{r}(s)$ to $\bar{\mathbf{r}}(\bar{s})$. The curves are parametrized by their respective arc lengths s and $\bar{s}$. In the transformed system, we require $\bar{\mathbf{e}}_i \cdot \bar{\mathbf{e}}_j = \delta_{ij}$, where $\bar{\mathbf{e}}_1 \equiv \bar{\mathbf{e}}_{\bar{x}}$ and $\bar{\mathbf{e}}_2 \equiv \bar{\mathbf{e}}_{\bar{z}}$ are the unit base vectors, thus introducing a new metric. That is, we are not dealing with a simple coordinate transformation leaving the metric properties of the plane unchanged, but we change the metric as well. Therefore, more care than usual is required as scalar products are not automatically preserved. Let θ and $\bar{\theta}$ denote the angles between the step's tangent and the average step direction in the Cartesian system and in the transformed system, respectively. They are related via

$$\tan\bar{\theta} = \frac{D_0\tan\theta}{D_{22} - D_{12}\tan\theta}. \quad (8)$$

The curvature in the transformed system is defined in the usual way, $\bar{\kappa} = \pm|\partial^2\bar{\mathbf{r}}/\partial\bar{s}^2|$; its sign is always the same as that of the Cartesian curvature. Finally, we introduce the gradient operator as $\bar{\nabla} = \bar{\mathbf{e}}_{\bar{x}}\partial_{\bar{x}} + \bar{\mathbf{e}}_{\bar{z}}\partial_{\bar{z}}$.

Under the above transformation the diffusion equation (3) becomes

$$\bar{D}_0\bar{\nabla}^2 c + F = \partial_t c, \quad (9)$$

with $\bar{D}_0 = D_0^2/D_{22}$. We have here achieved an interesting step, which is to suppress diffusion anisotropy. This is done, however, at a certain price: boundary conditions are affected by the transformation. The advantage lies in the fact that they keep the same form, albeit the effective step properties are now modified. Indeed the physical parameters Γ, $\nu_{\pm}$, and D_L are simply multiplied by a function of the orientation. More precisely, Eq. (4) becomes

$$\pm\bar{D}_0\bar{\mathbf{n}} \cdot \bar{\nabla}c|_{\pm} = \bar{\nu}_{\pm}(c - c_{\mathrm{eq}})|_{\pm}, \quad (10)$$

with $c_{\mathrm{eq}} = c_{\mathrm{eq}}^0[1 + \bar{\Gamma}(\bar{\theta})\bar{\kappa}]$. The normal vector $\bar{\mathbf{n}}$ is orthogonal to the tangent vector $\bar{\mathbf{t}} = \partial\bar{\mathbf{r}}/\partial\bar{\mathbf{s}}$ in the new metric. The step's normal velocities in the two coordinate systems are related via $\bar{v}_n\bar{\mathbf{n}} \cdot \mathbf{n} = v_n$, where the scalar product $\bar{\mathbf{n}} \cdot \mathbf{n}$ is evaluated in the Cartesian metric. The normal velocity in the transformed system becomes

$$\bar{v}_n = \Omega\bar{D}_0[\bar{\mathbf{n}} \cdot \bar{\nabla}c|_+ - \bar{\mathbf{n}} \cdot \bar{\nabla}c|_-] + a\partial_{\bar{s}}[\bar{D}_L\partial_{\bar{s}}(\bar{\Gamma}\bar{\kappa})]. \quad (11)$$

The parameters of the transformed model are defined as

$$\bar{\Gamma} = \frac{D_{22}\Gamma}{D_0}f(\bar{\theta})^3; \qquad \bar{\nu}_{\pm} = \frac{D_0\nu_{\pm}}{D_{22}f(\bar{\theta})}; \qquad \bar{D}_L = \frac{D_0D_L}{D_{22}}f(\bar{\theta});$$
$$f(\bar{\theta}) = D_0[(D_0\cos\bar{\theta} + D_{12}\sin\bar{\theta})^2 + D_{22}^2\sin^2\bar{\theta}]^{-1/2}, \quad (12)$$

where Γ, $\nu_{\pm}$, and D_L, which may be isotropic or anisotropic, are evaluated at the angle θ corresponding to $\bar{\theta}$ via Eq. (8). Equations (9)–(11) constitute a step model with isotropic terrace diffusion. Our program is now to solve the physical problems in this transformed frame and to map them back to the original physical coordinate frame.

We focus now on nonequilibrium step meandering, where the step will explore a wide range of orientations during its large meander. We show here that terrace diffusion anisotropy drastically affects the meandering scenario. We consider a vicinal surface with an average terrace width ℓ. For the sake of simplicity, we consider isotropic step properties and a one-sided model (i.e., $\nu_- = 0$ and $\nu_+ \to \infty$). Also, since the relaxation of the diffusion field is usually much faster than step motion, we shall use the quasistatic approximation, which amounts to setting $\partial_t c = 0$ in Eq. (9).

As shown originally by Bales and Zangwill [5], steps are morphologically unstable during growth, due to the presence of a Schwoebel effect (i.e., $\nu_- < \nu_+$). We consider a small perturbation of the step, of the form $\zeta(x, t) = \zeta_{\omega q}\exp[\omega t + iqx]$, where q is the wave number and ω is the complex growth rate of the perturbation. An instability is signaled by a positive real part of ω. The straight step is linearly unstable against perturbations of long enough wavelengths. One can also introduce a phase shift between the steps. It is then easily shown that the most unstable mode is the in-phase mode in the transformed frame. Hence, in the physical frame, the meander will lead to ripples with an angle $\phi_R = \arctan(D_{12}/D_{22})$,

as shown in Fig. 2. This is the first difference with meandering in the presence of step stiffness anisotropy or step edge diffusion anisotropy, where ripples are always perpendicular to the steps[6], i.e., $\phi_R = 0$.

The most unstable mode has a wavelength which is found to be given by

$$\lambda_m = 4\pi[\Gamma(D_S\bar{l} + D_L a)/(\Omega F\bar{l}^2)]^{1/2}, \qquad (13)$$

Here $D_S = D_0\Omega c_{\rm eq}^0$, and $\bar{l} = \ell D_0/D_{22}$. As displayed in Fig. 3, this wavelength is smaller as compared to an isotropic system with the same mean diffusion coefficient D_0 provided that the angle between the fastest direction and the average step orientation is smaller than a critical angle θ_c (obtained from the intersection between the curve in Fig. 3 and the horizontal line $\lambda_m/\lambda_m^{iso} = 1$). Indeed, the source of meandering instability is related to the fact that mass is transported along the steps from concave to convex parts of the steps. Therefore, when mass transport along the step is enhanced, the instability is stronger, and the wavelength is shorter. For small anisotropy, $\theta_c = \pi/4$; upon an increase of anisotropy, $\theta_c \to 0$. Hence, strong anisotropy has a stabilizing effect for all orientations, except when the step is almost perfectly aligned with the fast diffusion axis.

Following previous works [6–8], we perform a multiscale analysis by introducing slow spatial and temporal variables thanks to a small parameter ϵ proportional to the incoming flux F. We find the following highly nonlinear evolution equation for the step meander $\zeta(\bar{x}, t)$:

$$\partial_t\zeta = -\partial_{\bar{x}}\Big[\frac{\Omega F\bar{l}^2}{2}\,\frac{\partial_{\bar{x}}\zeta}{1+(\partial_{\bar{x}}\zeta)^2} - \Big(\frac{\bar{D}_S\bar{l}}{1+(\partial_{\bar{x}}\zeta)^2} + \frac{\bar{D}_L(\bar{\theta})a}{\sqrt{1+(\partial_{\bar{x}}\zeta)^2}}\Big)\partial_{\bar{x}}(\bar{\Gamma}(\bar{\theta})\bar{\kappa})\Big], \qquad (14)$$

where $\bar{D}_S = \bar{D}_0\Omega c_{\rm eq}^0$. Our problem is now very similar to that of Ref. [6], where line diffusion and step stiffness anisotropies have been accounted for. The main distinction is that the effective step properties now exhibit a twofold anisotropy [originated from terrace diffusion; see Eq. (12)], instead of fourfold anisotropy. According to the results reported in Refs. [6–10] (for an initial state corresponding to a straight step), we expect several general scenarios to emerge depending on the structure of the steady-state solutions: (i) A pattern takes place, and there is no coarsening when there is no steady-state solution with wavelength larger than λ_m. (ii) There is perpetual coarsening if and only if steady-state solutions exist for all wavelengths larger than λ_m. (iii) If the steady-state branch ceases to exist beyond a certain value $\tilde{\lambda} > \lambda_m$, then, generically, coarsening will stop around $\tilde{\lambda}$. For the set of parameters explored so far, we find that dynamics of Eq. (14) exhibit scenarios (i) and (iii).

For the sake of simplicity we assume that the principal axes are oriented along and perpendicularly to the average step direction. Then, the diffusion tensor reads

$$\underline{D} = D_0\begin{pmatrix}\alpha^{1/2} & 0\\ 0 & \alpha^{-1/2}\end{pmatrix}. \qquad (15)$$

If $\alpha < 1$, that is to say diffusion is faster in the z direction, stationary solutions with $\lambda > \lambda_c$ do not exist. Following the arguments in [6,8–10], we conclude that scenario (i) prevails. The wavelength is "frozen" and the amplitude of the meander increases without bound as $t^{1/2}$.

In the case where $\alpha > 1$, entailing that diffusion is faster in the x direction, we find stationary solutions above λ_c provided that line diffusion is present. Following the argument in [6,10], we conclude that the system obeys scenario (iii): The coarsening process is interrupted. However, in marked contrast to Ref. [6], the steady-state branch does not exhibit a maximum in the usual sense. Defining m_0 as the maximum value of $\sin(\theta)$ along a given periodic steady state of Eq. (14), we find that the steady-state wavelength λ increases monotonically up to the point where m_0 reaches its maximum value ($m_0 = 1$). At this point, λ reaches $\tilde{\lambda}$, whereby steady solutions cease to exist (Fig. 4). In the limit of pure line diffusion ($c_{\rm eq} = 0$) and for $\alpha \gg 1$, one finds that $(\tilde{\lambda}/\lambda_c) \sim \alpha^{1/2}$.

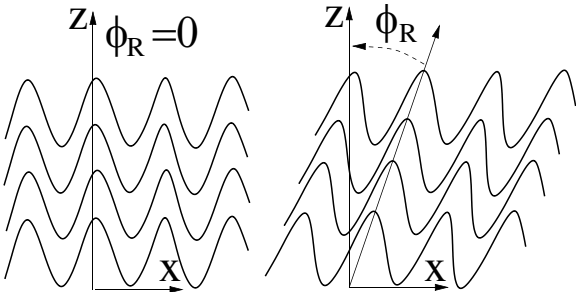

FIG. 2. Step meandering leads to ripples on a vicinal surface. In the presence of terrace diffusion anisotropy, ripples may be tilted with an angle ϕ_R.

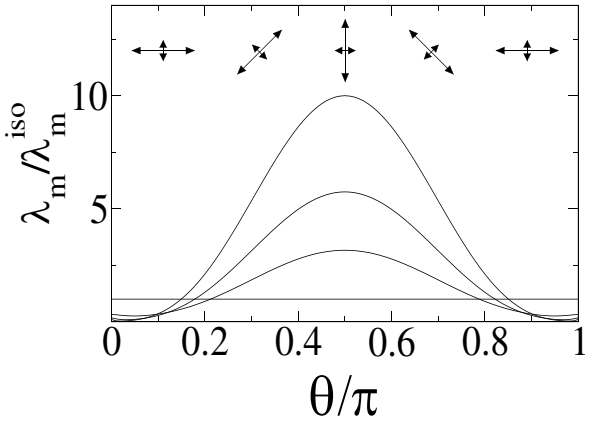

FIG. 3. The width of the meandering ripples corresponding to the most unstable mode [$\equiv \lambda_m\cos(\phi_R)$] as a function of the orientation of the anisotropy, for $\alpha = 1, 10, 30$, and 100.

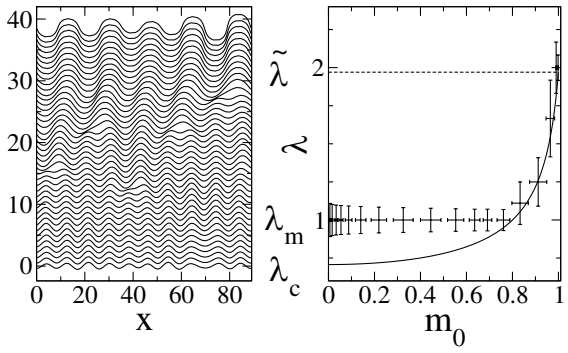

FIG. 4. Interrupted coarsening in the presence of terrace anisotropy. The left panel shows snapshots of the meander at different times (the amplitude has been arbitrarily rescaled for better visibility of the small fluctuations). The right panel shows the dynamics of the system in the λ-m_0 plane (average wavelength vs maximum slope). The line depicts the steady-state solutions of the evolution equation; the crosses show the evolution of the meander in the numerical simulation. Error bars indicate the standard deviation of λ and m_0. They are significant enough due to finite size effects. Parameters are $\alpha = 11$ and $c_{\mathrm{eq}} = 0$.

We have solved Eq. (14) numerically for various values of the parameters (Fig. 4). Coarsening is interrupted just above $\tilde{\lambda}$, and the system approaches the known asymptotic regime where the roughness of the meander increases as $t^{1/2}$ [8].

Let us now briefly mention that the present approach, based on geometrical mapping (7), may be relevant to other situations. Of particular interest is the application of this reasoning to study fluctuations with anisotropic terrace diffusion [11]. Statistical fluctuations can be added to a step model by means of Langevin forces [12]. Upon use of Eq. (7), a Langevin equation for step fluctuations can be derived with isotropic terrace diffusion. Once this goal is achieved, the correlation functions can be calculated [12]. The effect of terrace diffusion anisotropy is expressed via modification of the effective values of the step properties (such as $\bar{\nu}_{\pm}$ in the mapped model).

Another question that is worth mentioning pertains to the problem of denuded zones in submonolayer epitaxy on anisotropic substrates. At low coverage, the distance between islands is much larger than their size. The mapping presented here transforms this problem into an isotropic diffusion problem. Since islands are small, their shape and anisotropic properties do not matter, to leading order. Therefore, the "denuded zones," which correspond to the zone without other islands in the vicinity of a given island, are isotropic in the transformed frame. Going back to the physical frame, we straightforwardly obtain that the denuded zones must be elongated with an aspect ratio proportional to $(D_{\mathrm{fast}}/D_{\mathrm{slow}})^{1/2}$. This is indeed the result found in experiments and simulations [4]. Finally, the present work may also be useful regarding the extension to anisotropic diffusion of the results reported in Ref. [13] about second-layer nucleation.

What we have learned so far is that terrace diffusion induces nontrivial effects even upon a simple rotation of the main axes. Dynamics of steps are both qualitatively and quantitatively altered. Richness of anisotropic meandering dynamics ranges from patterns with frozen periodicity to interrupted coarsening, including the selection of tilted ripples. Besides the fundamental questions pertaining to nonequilibrium statistical physics regarding the birth of a variety of scenarios with a small number of parameters, this finding opens various inquiries in the field of design of templates for self-assemblies on vicinal surfaces.

This work is supported by the German-French cooperation program PROCOPE, Grants No. D/0122928 and No. 04643YK. Moreover, financial support by the Deutsche Forschungsgemeinschaft under Grant No. Em 68/3-1 is acknowledged.

[1] H. C. Jeong and E. D. Williams, Surf. Sci. Rep. **34**, 171 (1999); T. Ogino *et al.*, Surf. Sci. **514**, 1 (2002).
[2] M. Sato, M. Uwaha, Y. Saito, and Y. Hirose, Phys. Rev. B **67**, 125408 (2003).
[3] F. Buatier de Mongeot, G. Costantini, C. Boragno, and U. Valbusa, Phys. Rev. Lett. **84**, 2445 (2000).
[4] C. Ebner, K.-B. Park, J.-F. Nielsen, and J. P. Pelz, Phys. Rev. B **68**, 245404 (2003).
[5] G. S. Bales and A. Zangwill, Phys. Rev. B **41**, 5500 (1990).
[6] G. Danker, O. Pierre-Louis, K. Kassner, and C. Misbah, Phys. Rev. E **68**, 020601 (2003).
[7] F. Gillet, O. Pierre-Louis, and C. Misbah, Eur. Phys. J. B **18**, 519 (2000).
[8] O. Pierre-Louis, C. Misbah, Y. Saito, J. Krug, and P. Politi, Phys. Rev. Lett. **80**, 4221 (1998).
[9] S. Paulin, F. Gillet, O. Pierre-Louis, and C. Misbah, Phys. Rev. Lett. **86**, 5538 (2001).
[10] P. Politi and C. Misbah, Phys. Rev. Lett. **92**, 090601 (2004).
[11] M. Ondrejcek, W. Swiech, C. S. Durfee, and C. P. Flynn, Surf. Sci. **541**, 31 (2003).
[12] T. Ihle, O. Pierre-Louis, and C. Misbah, Phys. Rev. B **58**, 2289 (1998); S. Khare and T. L. Einstein, Phys. Rev. B **57**, 4782 (1998).
[13] P. Politi and C. Castellano, Phys. Rev. E **66**, 031606 (2003).